AJNR

Saccular Aneurysms on Straight and Curved Vessels Are Subject to Different Hemodynamics: Implications of Intravascular Stenting

H. Meng, Z. Wang, M. Kim, R.D. Ecker and L.N. Hopkins

AJNR Am J Neuroradiol 2006, 27 (9) 1861-1865
http://www.ajnr.org/content/27/9/1861

TECHNICAL NOTE

Saccular Aneurysms on Straight and Curved Vessels Are Subject to Different Hemodynamics: Implications of Intravascular Stenting

H. Meng
Z. Wang
M. Kim
R.D. Ecker
L.N. Hopkins

SUMMARY: Our aim was to examine hemodynamic implications of intravascular stenting in the canine venous pouch (sidewall or straight-vessel) and rabbit elastase (curved-vessel) aneurysm models. Flow dynamics in stented (Wallstent) and nonstented versions were studied by using computational fluid dynamics simulations and in vitro flow visualization, with a focus on stent placement effects on aneurysmal flow stagnancy and flow impingement. Results show that sidewall and curved aneurysm models have fundamentally different hemodynamics (shear-driven versus inertia-driven) and thus stent placement outcomes.

Saccular intracranial aneurysms generally occur at arterial curves and bifurcations in the circle of Willis,[1,2] with strong implication of a critical role for hemodynamics in such vascular geometry. Evaluations of endovascular interventions of aneurysms have relied on the venous pouch sidewall model in dogs[3,4] and the elastase curved-vessel model in rabbits.[5] Both models provide vessel dimensions similar to those in human cerebral arteries and afford easy microcatheter access.[6] However, the hemodynamic characteristics of these models have not been examined carefully, and little is known concerning how this lack of knowledge might affect the evaluation of intervention on these models. The purpose of the present study was to elucidate hemodynamic implications of stent placement in curved-versus-sidewall aneurysm models.

Methods

The canine model was abstracted as a sidewall spheric pouch on a straight vessel. The rabbit model was represented as a spheric pouch on a parent vessel segment with varying curves. Flow dynamics in these models were studied by using in vitro dye visualization and computational fluid dynamics (CFD) simulations. We then "treated" the models with a commercial porous intravascular stent and restudied them, focusing on the effects of stent placement on flow impingement and stagnancy of intra-aneurysmal flow.

In Vitro Flow Visualization Experiment

Two identical groups of elastomer aneurysm models, nonstented (control group) and stented (treatment group), with 4 different curvatures each (0 mm^{-1} straight vessel, S; 0.04 ± 0.01 mm^{-1}, C1; 0.08 ± 0.01 mm^{-1}, C2; and 0.1 ± 0.01 mm^{-1}, C3) were created[7] and used for in vitro flow visualization. This curvature range covers that typical of the rabbit elastase aneurysm model, based on models created at our center. Except for the parent vessel curvature, all geometric parameters (aneurysm diameter, neck size, vessel diameter, and angle of feeding and distal straight segments) remained constant (Fig 1*A*). Parent vessel curvature was defined as $C = 1/R$, R being the radius of the curvature of the vessel centerline in which the aneurysm was located. A self-expanding stent (5×40 mm; Wallstent, Boston Scientific, Natick, Mass) (Fig 1*B*) was deployed across the aneurysm neck in each of the 4 models in the treatment group.

The working fluid for the in vitro flow models was a 60/40 mixture of glycerin and water (attenuation, 1.157 g/cm^3; viscosity, 15.2 cP [1 cP = 0.001 Pa s]). A flow loop was set up as previously reported,[7] except that a height-adjusted tank was used to achieve steady flow. The flow rate was 375 mL/min; the corresponding Reynolds number (Re) was 128. The Dean number, defined as $\{(\Phi C/4)^{1/2}\mathrm{Re}\}$, where Φ is the diameter of the vessel lumen and C is the vessel curvature, ranged from 28–44 for the curved vessel models in our experiment. These values (thus the curvatures) were within the typical range found in human cerebral arteries (10–200).[8]

An optical dye (diluted stamp refill ink, Stockwell, Package Design Stockwell, Wesborough, Mass) was manually injected (6 mL of dye; injection rate, ~6 mL/s) near the aneurysm entrance to trace flow passing through the aneurysm. The models were oriented superiorly and posteriorly relative to respective parent vessels to examine the influence of orientation and possible gravity effect[7] on flow visualization. No significant changes were found between these 2 orientations, indicating negligible gravity effect with the optical dye. The flow in each orientation was recorded 3 times by a digital camera in a particle image velocimetry system (proVISION system, Integrated Design Tools, Tallahassee, Fla). The output resolution of the camera was 1360×1024 pixels. The recording frequency was 12 Hz; total recording time was approximately 15 seconds per acquisition.

Time-Intensity Curve Analysis and Stasis Index Calculation

To quantitatively characterize aneurysmal flow obtained from each acquisition of the in vitro flow image series, a time-intensity curve (TIC) was calculated. The stasis index (SI) was defined as the half-peak width of the TICs and was measured in seconds. The SI intuitively indicates the duration that dye remained in the region of interest.

CFD Simulations

CFD analysis was performed on a series of aneurysm models similar to those used in the flow-visualization experiment and under the same flow conditions as in that experiment. The vessel curvature was

Received October 3, 2005; accepted after revision April 23, 2006.

From the Toshiba Stroke Research Center (H.M., Z.W., M.K., R.D.E., L.N.H.) and the Departments of Neurosurgery (H.M., Z.W., M.K., R.D.E., L.N.H.) and Mechanical and Aerospace Engineering (H.M., Z.W., M.K.), University at Buffalo, State University of New York, Buffalo, NY.

This work was supported by: NIH/NINDS grant number one K25 NS047242, NIH/NIBIB grant number one R01EB002873, NIH/NIBIB grant number one R01NS43924, and NSF grant number BES-0302389.

Dr. Hopkins receives research and consultant support and has a financial interest in Boston Scientific Corporation.

Please address correspondence to: Hui Meng, PhD, Toshiba Stroke Research Center, State University of New York at Buffalo, 447 Biomedical Research Bldg, Buffalo, NY 14214; e-mail: huimeng@buffalo.edu

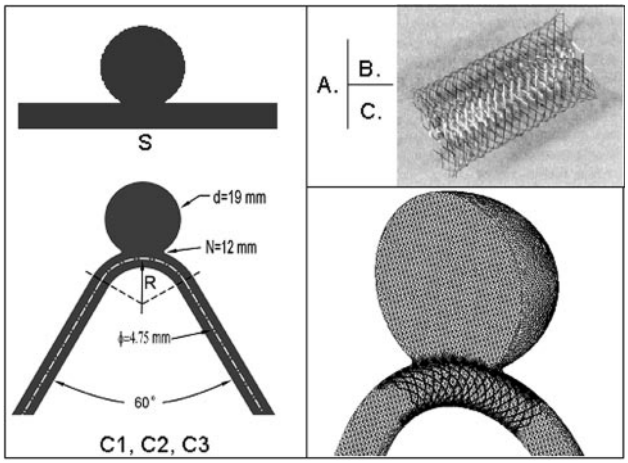

Fig 1. Aneurysm model geometry. *A,* Sidewall aneurysm on a straight vessel (S) and aneurysms on curved vessels with different curvatures (C1–C3). Curvature is defined as C = 1/R, where R is the radius of curvature of the parent vessel. N indicates neck size; d, aneurysm diameter; ϕ, vessel diameter. *B,* Stent used in the flow experiment and mimicked in the CFD simulations (5 × 40 mm Wallstent). *C,* Computational mesh in a stented aneurysm model used for CFD analysis.

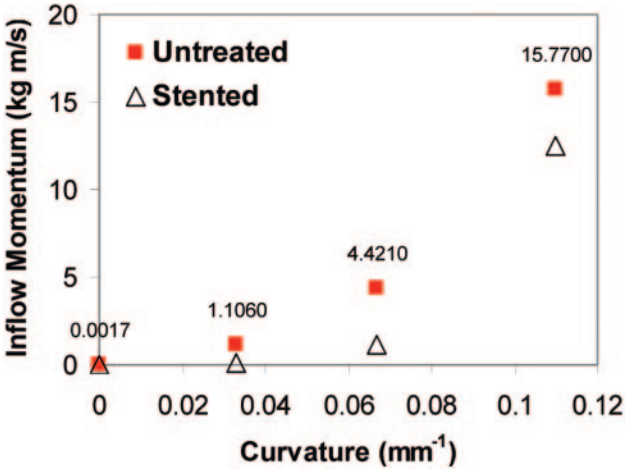

Fig 2. Inflow momentum as a function of vessel curvature (zero curvature corresponds to the sidewall aneurysm) from CFD simulation (Re = 128). Inflow momentum is calculated at the interface between the aneurysm orifice and parent vessel. The values for both untreated and stented models are calculated, but only the untreated models are labeled with values to show the difference between the straight vessel model (S) and the curved vessel (C) models.

$0\,mm^{-1}$ (S), $0.03\,mm^{-1}$ (C1), $0.07\,mm^{-1}$ (C2), and $0.11\,mm^{-1}$ (C3). A stent mimicking the Wallstent used in the flow experiment was simulated with the aid of computer-assisted design software (Pro-Engineering, PTC, Needham, Mass) (Fig 1*C*).

A steady-state flow condition was applied at the model inlet. Assumptions of Newtonian fluid, incompressible and laminar flow, and rigid wall were adopted. The CFD simulations were performed by using a commercial finite volume code (STARCD, Adapco, Melville, NY). Each stented model consisted of approximately 2.4 million tetrahedral meshes, and each nonstented model consisted of approximately 0.6 million tetrahedral meshes created by a software package (ICEM CFD, Ansys, Canonsburg, Pa) to achieve a stable solution. Mesh refinement tests were performed to achieve grid-independent simulation results. The CFD simulations provided 3D flow fields for each untreated and stented model.

Most CFD simulations were performed at the experimental flow condition of Re = 128. To evaluate how stent placement might affect wall shear stress (WSS) under a physiologically relevant flow condition, we also performed CFD simulations under higher flow (Re = 490), which matched the peak flow rate of a pulsatile flow at a patient's basilar artery measured with phase-contrast MR imaging (private communication, August 2002, University of Illinois Research Group, Chicago, Ill). Cerebral artery flow usually does not exceed an upper limit of Re = 600–700,[9] and Re values of 100, 400, and 700 have been used in a previous study.[10]

Hemodynamic Parameter Quantification from CFD Simulations

From the CFD flow field simulations, several hemodynamic parameters were calculated, including inflow momentum, WSS distribution, and impact zone. "Inflow region" was defined as the region at the interface between the aneurysm orifice and the parent vessel where flow velocity vectors pointed into the aneurysm. The "inflow momentum" was then calculated in the inflow region for each model. The WSS was calculated from the flow velocity gradient near the vessel wall by using the Newtonian fluid assumption. To quantify the influence of flow impingement at the distal neck of the aneurysm wall, we defined the "impact zone" as the area of the aneurysm wall where the WSS was elevated to >20 dynes/cm^2 for each model.[11]

Results

Flow Characteristics in Straight- and Curved-Vessel Aneurysm Models

There was a fundamental difference in flow mechanisms between the straight- and curved-vessel models. In the sidewall model, flow in the parent vessel was tangential to the aneurysm orifice. Its viscous force dragged a layer of fluid in the aneurysm to move along with it, resulting in a vortex in the aneurysm because of both the viscous shear force and confinement in the pouch. Being viscous shear-driven, the aneurysmal flow was relatively weak and sluggish.

In curved-vessel models, the aneurysm cavity was located along the inertial path of flow in the parent vessel. Inertial force drove flow into the aneurysm cavity. As curvature increased, the inertia-driven flow intensified and quickly dominated the aneurysmal flow field. These 2 distinct mechanisms are referred to as "shear-driven flow" and "inertia-driven" flow.

The 2 mechanisms brought about a significant difference in the strength of aneurysm flow. As vessel curvature increased from zero (straight model), inflow momentum drastically increased by several orders of magnitude (Fig 2; numbers above data points represent momentum for untreated models). From this result, we inferred that inertia-driven aneurysmal flow produced an inflow that was 10^3–10^4 times stronger than shear-driven flow.

Flow Modification Induced by Stent Placement

The shear-driven and inertia-driven flow mechanisms led to very different results after stent placement across the aneurysm orifice, as demonstrated by CFD and experiments:

Stent Placement Disrupted the Vortex Flow Pattern in the Sidewall Model but Not in Curved Aneurysm Models. In the sidewall model (Figs 3 and 4), the stent struts broke up the developing shear layer into small wells through which flow sieved (contour plot in Fig 3 insert). The shear-driven inflow that ordinarily entered from the distal neck was redistributed

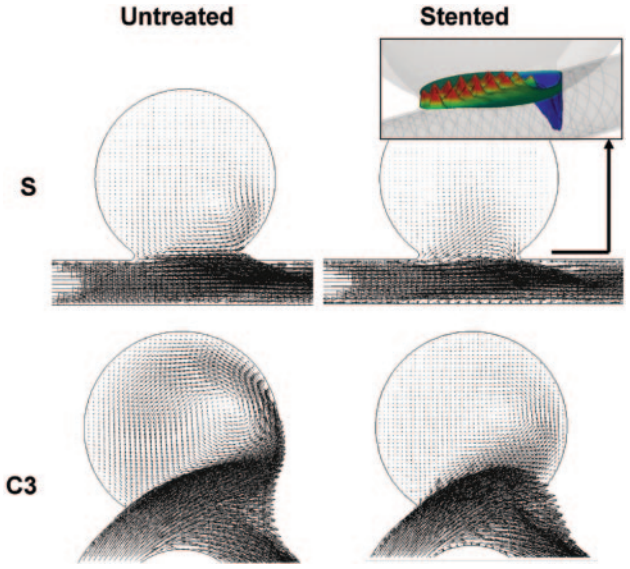

Fig 3. CFD simulation (3D) of aneurysmal flow in the straight vessel model (S) and one of the curved vessel models (C3) (Re = 128). Plotted are 2-dimensional velocity fields in the center plane. Insert reveals flow sieving through the stent struts in the straight vessel model. Shown is the vertical velocity magnitude contour at the aneurysm–parent vessel interface.

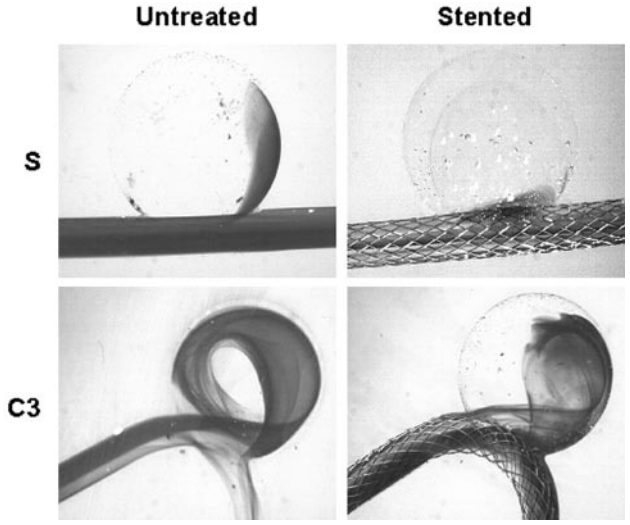

Fig 4. Dye visualization of the straight vessel model (S) and one of the curved vessel models (C3). The pictures are selected from the third image after the first appearance of dye in the aneurysm sac to represent the wash-in status.

across the orifice, and consequently, the counterclockwise aneurysmal vortex was disrupted by the stent. In contrast, in curved models, stent struts did not disrupt the overall inertia-driven inflow. Although the aneurysmal vortex was weakened by the stent placement, the counterclockwise vortex flow pattern remained nevertheless (Figs 3 and 4). Increasing vessel curvature among different curved models was associated with a stronger inflow jet and, hence, a stronger vortex with or without the stent.

Stent Placement Significantly Increased Flow Stagnancy in the Sidewall Models but Not in High-Curvature Aneurysm Models. Although stent placement increased flow stasis for each model, this increase diminished significantly with increasing vessel curvature (Fig 5). The increase in SI, measured in seconds, for various models, is given in the Table.

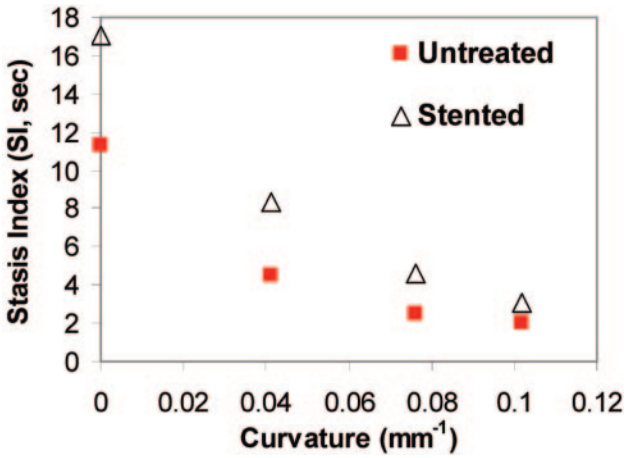

Fig 5. SI before and after stent placement as a function of vessel curvature for each model (S, straight; C, curved vessel) in the dye visualization experiment. As the curvature increases, SI decreases. Stent placement increases SI, but the increment is smaller in larger curvature models.

Effect of stenting on flow in sidewall (S) and curved (C) aneurysm models

Hemodynamic parameter change	Aneurysm Model			
	S	C1	C2	C3
Stasis index increase (s)	69	46	26	14
Inflow momentum reduction (%)	—	95	74	20
Impact zone reduction (%)	61	96	98	56

* Data correspond to Figures 2, 5, and 7.
† As an exception, the sidewall model (S) actually experienced an increase of inflow momentum due to an increased pressure drop along the vessel from stent placement under the fixed flow rate condition. The resulting inflow momentum was still significantly lower than in the curved models, untreated or stented, as can be seen in Figure 2.

Stent Placement Reduced Inflow Momentum in Curved Aneurysm Models. Inflow momentum was reduced after stent placement for each curved aneurysm model, but the reduction diminished as vessel curvature increased (Fig 2). The effect of stent placement on reduction of inflow momentum is further tabulated in the Table.

Stent Placement Reduced Impact Zone Under High Flow in All Aneurysm Models. Under the low-flow condition (Re = 128), the size of the impact zone at the distal wall did not show appreciable changes with curvature or stent placement. However, under the more physiologic high-flow condition (Re = 490), WSS levels and impact zone size experienced significant changes due to vessel curvature change or stent placement (Fig 6).

The size of the impact zone (WSS, >20 dynes/cm^2) on the wall was calculated and plotted against vessel curvatures (Fig 7). The impact zone was almost negligible for the untreated sidewall model but increased markedly with increasing curvature. Stent placement led to a dramatic reduction in the impact zone for all models: 61% for model S, 96% for model C1, 98% for C2, and 56% for C3 (listed in the Table). The percentage reduction of the impact zone in C3 (highest curvature) was lower than that in other models because the strong bend in the vessel rendered the stent to be less effective as a conduit for the flow in the parent vessel. As such, the jet shot in, resulting in impingement away from the neck region.

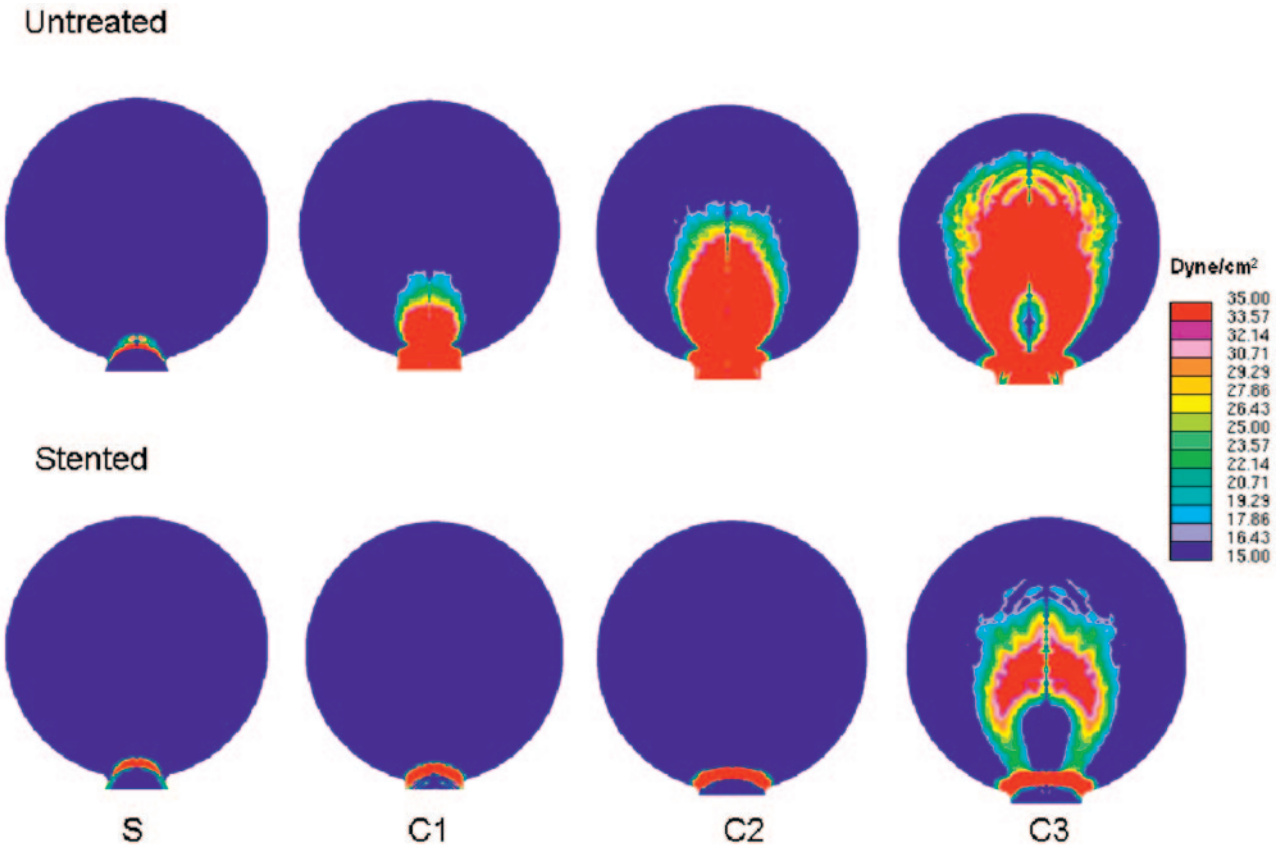

Fig 6. WSS distribution at the distal aneurysm wall and distal vessel wall in straight (S) and curved (C) models before and after stent placement, calculated from CFD simulation (Re = 490). Color scale represents WSS values from <15 dynes/cm^2 (deep blue) to >35 dynes/cm^2 (bright red). The impact zone is defined as the area where WSS is >20 dyne/cm^2, a value considered the upper limit for normal physiologic WSS.

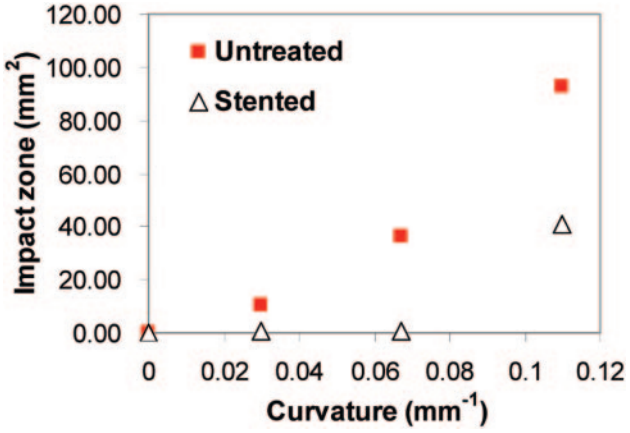

Fig 7. Impact zone for untreated and stented cases at various vessel curvatures, calculated from CFD simulation (Re = 490). The stent disturbs more impinging flow to decrease the impact zone at the moderately curved vessel, but the stent effect diminishes at the highly curved vessel.

Discussion

During the past decade, stand-alone stent placement has been explored as an alternative intervention, with the hope that stent struts would disrupt aneurysmal flow sufficiently to cause blood stasis that would lead to thrombotic occlusion of the aneurysm.[12-19] However, most investigations were based on the canine model or its abstraction—sidewall aneurysms on straight vessels, which rarely occur in human intracranial aneurysms. Also lacking is how stent placement—alone or in combination with coiling—affects hemodynamic stresses and the resultant vascular remodeling process.

Diminished Potential of Stent Placement for Thrombotic Occlusion of Aneurysms on Curves and Bifurcations

Our results have shown that the stent-induced flow reduction diminished with increasing vessel curvature. In the sidewall model, shear-driven flow is already considerably more sluggish than the inertia-driven flow in aneurysms on curves, even before stent placement. Hence, a porous stent could easily disrupt the aneurysmal vortex and create stasis in the canine aneurysm (as reported in numerous descriptions of successful thrombotic occlusion of sidewall aneurysm models).[3,4] In our curved models, however, the aneurysmal vortex flow pattern remained despite stent placement. Furthermore, as vessel curvature increased, stent-induced flow stagnancy decreased, with the highest flow reduction experienced in the sidewall model. Thus, the potential for stent-induced thrombotic occlusion was diminished for aneurysms on curves. The same can be expected from bifurcation aneurysms because the flow in these aneurysms is also inertia-driven.

More Protective Roles of Stents in Aneurysms on Curves or at Bifurcations

We found that Wallstent placement in curved-vessel aneurysm models drastically reduced inflow momentum, WSS, and impact zone size at the distal wall. Thus, we submit that stent placement can play additional therapeutically protective

roles besides the usually expected role for potential thrombotic occlusion:

Encouraging Favorable Remodeling—Slowing Down or Stopping Aneurysm Growth and Possibly Decreasing Rupture Risk. The impact zone, experiencing higher-than-normal WSS, is likely the active site for initiating wall degradation and aneurysm growth.[11] By reducing WSS to the physiologic range and cutting down the impact zone,[20] the stent could encourage favorable wall remodeling and potentially stabilize the aneurysm, thereby decreasing rupture risk.

Reducing Coil Compaction and Aneurysm Regrowth. Stent placement has been used widely to assist coiling in cerebral aneurysm treatments. We have shown that a commercial porous stent such as the Wallstent can significantly reduce the inflow momentum. Therefore, we suggest that in addition to serving as a scaffold to contain coils, the stent can weaken the impinging force exerted on the coil mass and thereby reduce coil compaction This may further discourage aneurysm regrowth.

Animal Models for Evaluating Endovascular Intervention

Among animal models for endovascular intervention evaluation, the canine venous pouch model and the rabbit elastase model are most frequently used. In the present study, these were abstracted as the straight-vessel (sidewall) model and the curved vessel model, respectively. The rabbit elastase model is anatomically closer to human cerebral aneurysms.[6,21] Consistent with the histology of human intracranial aneurysms, the elastase-created aneurysm wall has a disrupted or disappearing internal elastic lamina, a thinned tunica media, and some limited inflammatory cell deposition and thrombosis. The vessel diameter in the rabbit model approximates that of the middle cerebral artery in humans, and the blood pressure and coagulation system are similar as well. Conversely, the canine model is simpler to create and thus still widely used.[22,23] To our knowledge, no study has examined the hemodynamic implications of placing a stent on a curved-versus-straight vessel with a saccular aneurysm.

We have shown distinct flow mechanisms between the 2 types of aneurysm geometries, which lead to different flow modifications after stent placement. The canine model might give a false-positive indication of the stent inducing thrombotic occlusion. A model capturing the vessel geometry (on a curve, at a bifurcation, or both) of human cerebral aneurysms will give more reliable hemodynamic indication of endovascular intervention results. In this sense, our hemodynamic study further supports that the rabbit elastase model is a more realistic aneurysm model than the canine model.

Acknowledgment

We thank Scott Woodward for stimulating discussions.

References

1. Stehbens WE. **Pathology and pathogenesis of intracranial berry aneurysms.** *Neurol Res* 1990;12:29–34
2. Weir B. **Unruptured intracranial aneurysms: a review.** *J Neurosurg* 2002;96:3–42
3. Geremia G, Haklin M, Brennecke L. **Embolization of experimentally created aneurysms with intravascular stent devices.** *AJNR Am J Neuroradiol* 1994;15:1223–31
4. Wakhloo AK, Schellhammer F, de Vries J, et al. **Self-expanding and balloon-expandable stents in the treatment of carotid aneurysms: an experimental study in a canine model.** *AJNR Am J Neuroradiol* 1994;15:493–502
5. Cloft HJ, Altes TA, Marx WF, et al. **Endovascular creation of an in vivo bifurcation aneurysm model in rabbits.** *Radiology* 1999;213:223–28
6. Powell J. **Models of arterial aneurysm: for the investigation of pathogenesis and pharmacotherapy—a review.** *Atherosclerosis* 1991;87:93–102
7. Wang ZJ, Hoffmann KR, Wang Z, et al. **Contrast settling in cerebral aneurysm angiography.** *Phys Med Biol* 2005;50:3171–81
8. Niimi H, Kawano Y, Sugiyama I. **Structure of blood flow through a curved vessel with an aneurysm.** *Biorheology* 1984;21:603–15
9. Liepsch DW, Steiger HJ, Poll A, et al. **Hemodynamic stress in lateral saccular aneurysms.** *Biorheology* 1987;24:689–710
10. Danturthi R, Partridge LD, Turitto VT. **Hemodynamics of intracranial lateral aneurysms: flow simulation studies.** *Proceedings of the 16th Southern Biomedical Engineering Conference. Biloxi, Mississippi,* April 1997:224–27
11. Hoi Y, Meng H, Woodward SH, et al. **Effects of arterial geometry on aneurysm growth: three-dimensional computational fluid dynamics study.** *J Neurosurg* 2004;101:676–81
12. Lanzino G, Wakhloo AK, Fessler RD, et al. **Efficacy and current limitations of intravascular stents for intracranial internal carotid, vertebral, and basilar artery aneurysms.** *J Neurosurg* 1999;91:538–46
13. Lylyk P, Cohen JE, Ceratto R, et al. **Endovascular reconstruction of intracranial arteries by stent placement and combined techniques.** *J Neurosurg* 2002;97:1306–13
14. Liou TM, Liou SN, Chu KL. **Intra-aneurysmal flow with helix and mesh stent placement across side-wall aneurysm pore of a straight parent vessel.** *J Biomech Eng* 2004;126:36–43
15. Rhee K, Han MH, Cha SH. **Changes of flow characteristics by stenting in aneurysm models: influence of aneurysm geometry and stent porosity.** *Ann Biomed Eng* 2002;30:894–904
16. Yu SC, Zhao JB. **A steady flow analysis on the stented and non-stented sidewall aneurysm models.** *Med Eng Phys* 1999;21:133–41
17. Lieber BB, Gounis MJ. **The physics of endoluminal stenting in the treatment of cerebrovascular aneurysms.** *Neurol Res* 2002;24(suppl 1):S33–42
18. Ohta M, Hirabayashi M, Wetzel S, et al. **Impact of stent design on intra-aneurysmal flow.** *Intervent Neuroradiol* 2004;10:85–94
19. Stuhne GR, Steinman DA. **Finite-element modeling of the hemodynamics of stented aneurysms.** *J Biomech Eng* 2004;126:382–87
20. Glagov S. **Intimal hyperplasia, vascular modeling, and the restenosis problem.** *Circulation* 1994;89:2888–91
21. Abruzzo T, Shengelaia GG, Dawson RC 3rd, et al. **Histologic and morphologic comparison of experimental aneurysms with human intracranial aneurysms.** *AJNR Am J Neuroradiol* 1998;19:1309–14
22. Klisch J, Schellhammer F, Zitt J, et al. **Combined stent implantation and embolization with liquid 2-polyhydroxyethyl methacrylate for treatment of experimental canine wide-necked aneurysms.** *Neuroradiology* 2002;44:503–12
23. Shin YS, Niimi Y, Yoshino Y, et al. **Creation of four experimental aneurysms with different hemodynamics in one dog.** *AJNR Am J Neuroradiol* 2005;26:1764–67